CHEMISTRY
A EUROPEAN JOURNAL

DOI: 10.1002/chem.200801129

Fluorescent Magnesium(II) Coordination Polymeric Hydrogel

Wei Lee Leong, Sudip K. Batabyal, Stefan Kasapis,* and Jagadese J. Vittal*[a]

Abstract: A pH and mechano-responsive coordination polymeric gel was developed without the use of long chain hydrophobic groups. The hydrogel was synthesised by reacting the aqueous solution of Mg^{2+} with the basic aqueous solution of *N*-(7-hydroxyl-4-methyl-8-coumarinyl)-alanine. The gelation is attributed to the self-aggregation of 1D coordination polymers to form 3D nanostructures through non-covalent interactions to entrap water molecules. The freeze-dried hydrogel exhibits a fibrillar network structure with a uniform ribbon shape. UV/vis absorption studies illustrate that the hydrogel displays a typical π–π^* transition. The fluorescence intensity of the hydrogel is enhanced drastically with a longer lifetime upon gel formation. Mechanical analysis including dynamic oscillation on shear, steady shear and creep (retardation-relaxation) testing have been performed to elucidate the supramolecular nature of the 3D assembly. Together with the viscoelastic properties and biocompatibility, the Mg^{2+} hydrogel may find utility as a novel soft material in biomedical applications.

Keywords: coordination polymers · fluorescence · hydrogel · magnesium · viscoelasticity

Introduction

The supramolecular gels derived from organic molecules have gained considerable attention, owing to their unique features and versatile applications as soft materials.[1] Nevertheless, metallogels and coordination polymeric gels are of emerging research interest.[2] The metal coordination to a gelator would give rise to intriguing spectroscopic, catalytic[3] and redox[4] properties of the gel-phase materials. Thus, a lot of effort has been devoted to investigating the spectroscopic properties of metallo- and coordination polymeric gels. For instance, a class of heat-set gel-like networks formed by Co^{2+} complexes of 4-alkylated 1,2,4-triazole has shown thermochromic behaviour during the phase transition.[5] Thermochromic and reversible colour change behaviour has been observed during the sol–gel transition of a gel derived from Cu^{+} bipyridyl derivative of cholesteryl.[4] Phenylalanine-based bolaamphiphile metallogels have found application in water purification and a vitamin B_{12} carrier based on their absorption properties.[6] Such interesting absorption studies have driven the research on the photoluminescence properties of metallo- and coordination polymeric gels. Recently, 8-quinolinol derivatives have been reported to form metallogel with Cu^{2+}, Pd^{2+} and Pt^{2+}. Interestingly, the Pt^{2+} complex exhibits unique thermo- and solvatochromism of visible and phosphorescent colour during sol–gel phase transition.[7] A phosphorescent Au^{+} pyrazolate gel showed reversible colour switching upon sol–gel transition and doping/dedoping of Ag^{+}.[8] Rowan's group reports the gel formation of 2,6-bis(benzimidazolyl)-4-hydroxypyridine derivative of pentaethylene glycol in the presence of lanthanide and transition metal ions, which exhibits photoluminescence, owing to the "antenna effect" of Eu^{3+}.[9] Alkylated platinum terpyridyl systems have been found to form organogel, owing to metal–metal and π–π interactions and the metallogels show drastic emission changes during the sol–gel transition.[10] Platinum acetylide organogelators exhibit phosphorescence in solution and in the aggregate/gel state, owing to triplet-triplet energy transfer.[11]

Recently we have reported that coumarin derivatised glycine (H_2mugly: *N*-(7-hydroxyl-4-methyl-8-coumarinyl)-glycine) gelates water instantly upon addition of Zn^{2+}.[12] The Zn^{2+} coordination polymeric gel shows fluorescence enhancement upon hydrogelation. This interesting finding has prompted us to explore the utilization of the main group metals in coordination polymeric gel synthesis. In contrast to transition and post-transition metals, which often quench the fluorescence due to the electron or energy transfer be-

[a] W. L. Leong, Dr. S. K. Batabyal, Prof. S. Kasapis, Prof. J. J. Vittal
Department of Chemistry, National University of Singapore
3 Science Drive, 117543 (Singapore)
Fax: (+65) 6779-1691
E-mail: chmsk@nus.edu.sg
chmjjv@nus.edu.sg

Supporting information for this article is available on the WWW under http://dx.doi.org/10.1002/chem.200800xxx.

tween the metal cations and fluorophores,[13] main group metals do not quench the fluorescence. It has been reported that the fluorescence properties of coumarin derivatives can be retained in the presence of alkali-earth metals and quenched by transition metals.[14] The main group metals, particularly Mg^{2+}, are essential minerals in the biological systems. Mg^{2+} is the most abundant of the divalent ions in cells, and plays an important role in cell proliferation and cell death. It also participates in the modulation of signal transduction, various transporters, and ion channels.[15] On the other hand, it has been reported that hydrogelators based on amino acids[16] and some hydrogels have been demonstrated as biocompatible materials.[16f–l] Thus, it would be of interest to incorporate Mg^{2+} ions in the preparation of biocompatible and stimuli responsive amino acid-based metallogel. A biocompatible hydrogel provides an alternative candidate for drug delivery[17] and tissue engineering.[17d,18]

Mechanical properties constitute a critical consideration in practical use of such soft materials, and appropriate rheological techniques have been utilised to probe the viscoelastic and mechano behaviour of the supramolecular gels.[9b,19] Here we report the hydrogelation of Mg^{2+} coordination polymer of a coumarin derivatised alanine (**1**, H_2muala: *N*-(7-hydroxyl-4-methyl-8-coumarinyl)-L-alanine). The microscopic morphology of the freeze-dried gel has been investigated by using scanning electron microscopy (SEM) and transmission electron microscopy (TEM) techniques. Photopysical properties of the complex and the corresponding gel have been studied in detail. Rheological studies have been performed to elucidate the small and large deformation viscoelasticity of the gel.

Results and Discussion

In our recent study,[12] H_2mugly has been developed as suitable hydrogelator with Zn^{2+} without the use of long chain hydrophobic groups. No such gelation was observed if the structurally similar H_2muala **1** (Scheme 1) was used. This observation suggests that the substituent on the amino acid side chain may not change the overall coordination and conformation of the complex, however, it would influence the supramolecular interactions leading to gelation.

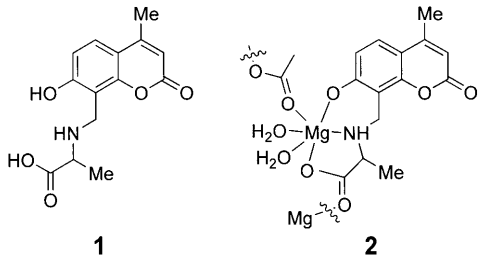

Scheme 1. Structure of the ligand **1** and schematic representation of the proposed Mg^{2+} coordination polymer **2**.

In this study, **1** has been observed to form hydrogel with Mg^{2+} upon mixing. If a basic aqueous solution of **1** is reacted with an aqueous solution of $Mg(CH_3COO)_2{\cdot}4H_2O$, a yellow clear solution is formed initially. If the solution mixture was left undisturbed at room temperature for about 20 min, an opaque gel of $[Mg(muala)(H_2O)_2]{\cdot}nH_2O$ **2** (27 wt%, Scheme 1) was obtained. Gel formation is confirmed by the inverted test tube method (Figure 1). No such gelation was observed if the same reaction was repeated with other organic solvents (including MeOH and EtOH) or Ca^{2+}. The powder of **2** can be obtained by slow evaporation from a methanolic solution. Further analysis and characterization were conducted with the powdered sample unless otherwise mentioned. Complex **2** is a neutral compound with a metal to ligand ratio of 1:1, as evidenced from the elemental analysis and Job's plot. The water molecules found from elemental analysis differ from the number of their counterparts associated with the gelator in the hydrogel. This should be attributed to the difference of solvents present in the solid (MeOH) and gel (H_2O) state.

Figure 1. The photograph of ligand **1** (left) and hydrogel **2** (right).

The hydrogel converts to a yellowish clear solution at pH 2, but retains its gel structure at pH 8 indicating pH responsive properties. Under the acidic conditions, the ligand **1** is protonated and thereby disturbs the complexation and, hence, the gel structure. The hydrogel also exhibits mechano responsive behaviour in which it can recover the gel structure on standing, following vigorous shaking to fluidise. The gel is soluble in common organic solvent like methanol, ethanol, THF and DMF. Slow evaporation of the diluted methanolic solution of the gel gave a free standing polymeric film (see the Supporting Information).

We propose that **2** is a 1D coordination polymer with the carboxylate O of the ligand coordinating the neighbouring Mg^{2+} centre as supported by FT-IR absorption studies. The difference in asymmetric ($\tilde{\nu}_{as}$) and symmetric ($\tilde{\nu}_s$) stretching frequencies of carboxylate group in freeze dried **2** was found to be 114 cm^{-1}, suggests the bridging coordination mode of the carboxylate groups (see the Supporting Information). In general, $\Delta\tilde{\nu}$ reflects the coordination geometry of carboxylate, in which $\Delta\tilde{\nu} > 200\ cm^{-1}$ for the monodentate carboxylate and $\Delta\tilde{\nu} < 200\ cm^{-1}$ for bridging carboxylate.[20]

Nonetheless, in the absence of crystal structure, the monomeric species cannot be ruled out. Postulation of a 1D coordination polymeric structure can easily explain the gel formation in which the 1D polymeric strands entangle with each other to form a 3D fibrous network. The water molecules are entrapped within the porous network and form a stable hydrogel. It appears that entanglement of the nanofibre gel network takes place as a result of hydrogen bonding between amino and carboxylate groups in the ligand, and water molecules. The disk-like coumarin rings are expected to assemble in order to form hydrophobic pockets.

Hydrogel **2** exhibits different properties as compared to the previously reported gelation of Zn^{2+} with H_2mugly.[12] The gelation process observed here requires about 20 min at room temperature to occur, whereas Zn^{2+} forms a gel instantly upon mixing with the ligand. Conversely, a higher concentration of gelator is required for gel formation, as compared to the Zn^{2+} coordination polymeric gel. Furthermore, these two gels have different thermal properties. Upon heating to 65°C, the Zn^{2+} gel becomes a white precipitate and the gel structure does not recover upon cooling. For Mg^{2+} gel, upon heating to the same temperature, it turns to a clear yellow solution and upon cooling, the gel structure is visually restored.

Morphological studies of hydrogel: The morphology of hydrogel **2** was investigated by using SEM and TEM. The investigation reveals that the hydrogel **2** is formed by the self assembled fibrous structure of the coordination polymer. Figure 2a exhibits the typical low magnification field emission SEM micrograph of freeze dried **2**, which reveals the fibrillar-network structure of the gel. The higher magnification image (see the Supporting Information) shows that these fibres are quite uniform ribbon shaped with a rectangular cross-section. These fibres are several micrometers long and the diameters are in the range of 50–150 nm. It seems that the coordination polymeric chains of the Mg^{2+} complex are bundled up to self-assemble into a fibrous network. TEM analysis also supports the concept of the gel being composed of micro-sized tapes, which are several microns long (Figure 2b) and the diameters are in the range of 50–100 nm. Furthermore, the high resolution TEM micrographs of these ribbons indicate a predominant amorphous nature. Thus, no crystal fringe patterns were observed and the electron diffraction patterns exhibit diffuse rings suggestive of amorphous microstructures (see the Supporting Information).This amorphous behaviour is different from that found in the zinc(II) coordination polymeric gel containing a similar ligand.[12]

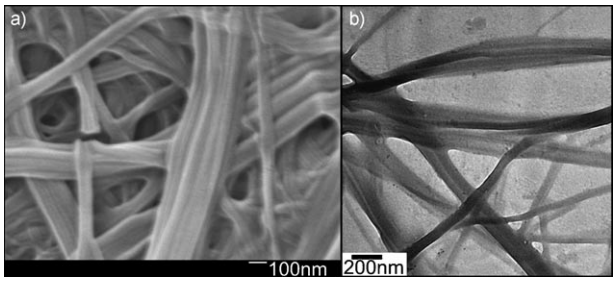

Figure 2. Electron micrograph of freeze dried **2**: a) SEM image; b) TEM image.

Photophysical studies: The absorption and emission properties of **1** and **2** were studied extensively. Upon addition of Mg^{2+} ions to an aqueous solution of **1** in the presence of two equivalents LiOH ($[\mathbf{1}]=1.04\times10^{-4}$ M), a typical π–π* absorption band appears at 360 nm.[21] The 1:1 complexation model for Mg^{2+} ion-binding was elucidated by a Job's plot (see the Supporting Information). Upon addition of Mg^{2+} ions to an aqueous solution of **1**, hydrogel **2** was formed after 20 min. The UV/vis spectral traces of **1**, hydrogel **2** and sol **2** ([**1**] and [**2**] = 50 mM) are shown in Figure 3. No shifting in the absorption energy was observed for hydrogel **2**. The addition of concentrated HCl to hydrogel **2** turns it into the sol state. The π–π* absorption band of sol **2** shows a large blue shift in energy to $\lambda=320$ nm.

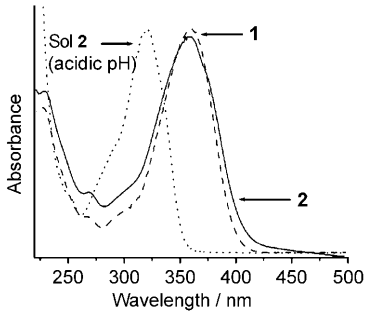

Figure 3. UV/vis absorption of **1** in H_2O, hydrogel **2** and its corresponding sol state in acidic medium ([**1**] and[**2**] = 50 mM). The samples were sandwiched between quartz plates.

As hydrogel **2** is pH dependent, absorption studies of **1** in the presence of one equivalent of Mg^{2+} ($[\mathbf{1}]=1.04\times10^{-4}$ M) have been investigated in buffer solutions at various pH. It has been reported that in neutral or weakly acidic solutions, 7-hydroxycoumarin derivatives are in the neutral form, which absorbs near $\lambda=320$ nm. In alkaline solution, 7-hydroxycoumarin derivatives are in the tautomeric form and show a marked bathochromic shift to $\lambda=360$ nm.[21] The UV/vis absorption spectra of **1** at various pH in buffer solutions also exhibit a similar behaviour, in which a π–π* absorption band appears at $\lambda=320$ nm in acidic conditions and shifts to $\lambda=360$ nm in alkaline solution (see the Supporting Information). Likewise, the Mg^{2+}-bound species exhibit the same trend, as shown in Figure 4a. This suggests that an acidic medium would cause protonation of the ligand, hence leading to dissociation of the complex.

To study the effect of temperature on hydrogel **2**, variable-temperature UV/vis absorption studies have been carried out from 15–85°C ([**2**] = 50 mM). The UV/vis spectral

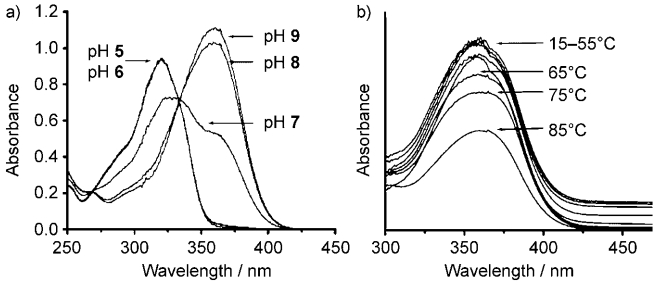

Figure 4. a) UV/vis absorption spectra of **1** in the presence of one equiv of Mg^{2+} ($[\mathbf{1}]=1.04\times10^{-4}$ M) at various pH in buffer solutions; b) hydrogel **2** ($[\mathbf{2}]=50$ mM) at various temperatures (sample sandwiched between quartz plates).

traces of hydrogel **2** at different temperatures are shown in Figure 4b. At 25°C, an absorption band at $\lambda=360$ nm was observed, which corresponds to the π–π* absorption band characteristic of the Mg^{2+}-bound species. No significant spectral changes were observed upon increasing temperature to 55°C. Further increasing the temperature resulted in a drastic drop in absorbance. This reflects in that the hydrogel **2** is stable at temperatures below 55°C, but becomes unstable at higher temperatures. This is in correlation with the aforementioned thermal properties of hydrogel **2**, which melts around 65°C.

The fluorescence spectral traces of basic aqueous **1** and hydrogel **2** ($[\mathbf{1}]$ and $[\mathbf{2}]=50$ mM) upon excitation at $\lambda=$ 360 nm are shown in Figure 5a. The hydrogel **2** exhibits strong blue emission with maxima at $\lambda=455$ nm. The fluorescence intensity has been enhanced drastically, as compared to **1**. The photoluminescence of hydrogel **2** can be visualised by naked eye under UV light. Moreover, blue luminescence emitted from nanoribbon can be directly observable under a fluorescence microscope (see the Supporting Information).

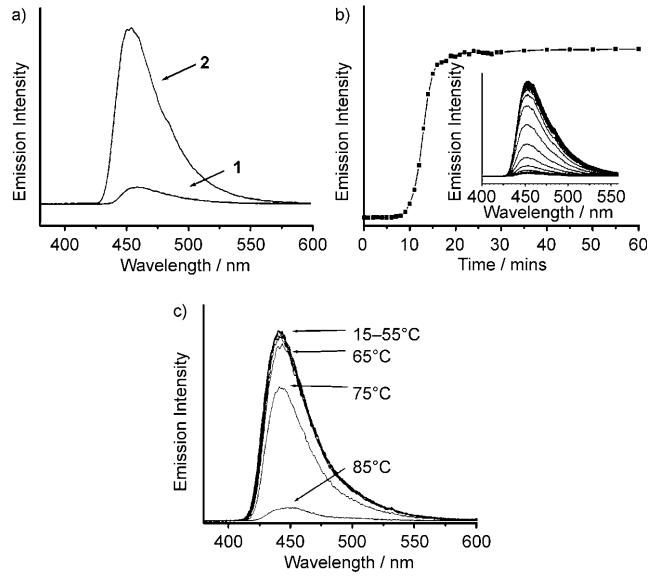

Figure 5. a) Emisssion spectra of **1** and hydrogel **2** ($[\mathbf{1}]$ and $[\mathbf{2}]=50$ mM) upon excitation at $\lambda=360$ nm; b) Time-dependent emission intensity of hydrogel **2** at $\lambda=455$ nm. The inset shows the fluorescence spectral traces against time; c) Fluorescence spectra of hydrogel **2** at different temperatures.

Controlled experiments were conducted to investigate whether the fluorescence enhancement is owed to the hydrogel formation or complexation with Mg^{2+}. The emission properties of the basic aqueous solution of **1** ($[\mathbf{1}]=1.04\times10^{-4}$ M) upon addition of Mg^{2+} were studied. There is no significant change in fluorescence intensity was observed upon excitation at $\lambda=360$ nm. This finding indicate that complexation of Mg^{2+} ions with **1** in solution did not result in a fluorescence enhancement, as compared to free ligand **1**. Furthermore, controlled experiment with Ca^{2+} in place of Mg^{2+} does not exhibit such drastic fluorescence enhancement, suggesting that the enhancement is due to the formation of hydrogel **2** (see the Supporting Information).

As the hydrogel **2** forms over a period of time, time-dependent emission studies have been performed to investigate effect of gelation on the fluorescence behaviour. Figure 5b displays the fluorescence intensity of **2** at $\lambda=445$ nm during the gelation process. It can be seen that the fluorescence intensity increases and reaches a constant value at $t\approx20$ min, that is, at a time coincident with gel formation. There is no more increment in fluorescence intensity at longer times of experimentation. This indicates that the maximum fluorescence intensity is only observed if the hydrogel **2** is completely formed. The enhancement of fluorescence intensity upon formation of coordination polymeric gel was also noted previously.[12] Such fluorescence enhancement in the gel state compared to the sol state also has been reported for low molecular mass gels[22] and two-component gels.[23] Generally, an increase in the rigidity of a molecule can decrease molecular vibrations, probably suppress the internal conversion of an excited molecules, and may increase the fluorescence quantum yield.[24]

Variable-temperature fluorescence spectral traces of hydrogel **2** are shown in Figure 5c. No significant spectral changes were observed as the temperature was increased from 15–55°C. There is a slight decrease in fluorescence intensity if hydrogel **2** was heated to 65°C. Further increment of temperature resulted in decreasing the emission. The results suggest that the emission of hydrogel **2** decreases as it starts to melt at 65–75°C. These findings indicate that optimal emission of **2** is when the hydrogel is completely formed and that the emission of the hydrogel decreases as it melts at higher temperature. This striking observation should be attributed to the rigidification of the media upon gelation, a process that slows down nonradiative decay mechanisms hence leading to luminescence enhancement.[24] Though the hydrogel dissociates from aggregation state and shows a drastic drop in fluorescence intensity, the complex still exhibits a considerable blue emission in the solution state. This could be attributed to the presence of weak supramolecular interactions whilst still in the solution state.

Further studies have been done to gain insight of luminescence properties of hydrogel **2**. The emission decay profiles

were monitored at $\lambda = 450$ nm for a basic aqueous solution of **1** and hydrogel **2** (see the Supporting Information). The fluorescence decay of **1** was fit well with a single exponential component yielding a lifetime of 2.75 ns($\pm$0.07 ns). Analysis of the emission decay profile of **2** gave a longer lifetime of 3.44 ns($\pm$0.03 ns). It reflects that the formation of hydrogel in its aggregate state increases the rigidity and restricts the rotational and vibrational movements of molecules. The limited molecular motions decrease the nonradiative relaxation process, which leads to the longer lifetime and fluorescence enhancement.[24]

Mechanical properties of the networks formed: The mechanical properties of the three dimensional structure of hydrogel **2** was performed by using small and large deformation dynamic oscillation, steady shear and transient (creep) measurements. The linear viscoelastic region (LVR) of hydrogel **2**, as a function of increasing amplitude of deformation on shear, was determined with a strain amplitude ranging from 0.01 % to 200 % at 1 rad s^{-1} (Figure 6a). Both the in-phase storage modulus (G') and out-of-phase loss modulus (G'') remain constant up to $\approx$1 % strain ($G' > G''$), an outcome which defines the uppermost bound of LVR. Beyond this level of deformation, a catastrophic disruption of the network occurs as indicated by the steep drop in the values of both moduli and the reversal of the viscoelastic signal ($G'' > G'$). From these data it was decided to perform subsequent measurements on the gel at 0.1 % strain, which lies comfortably within LVR.

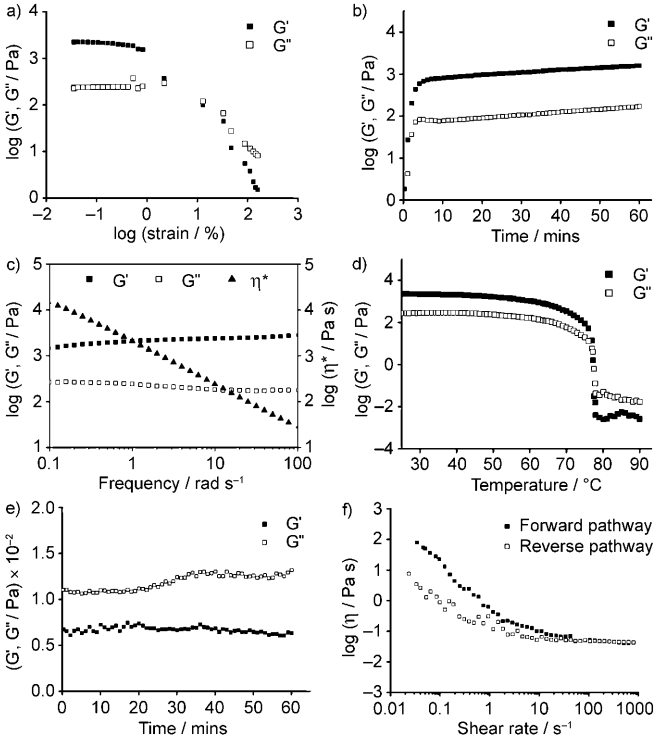

Figure 6. Dynamic oscillatory and steady shear measurements of hydrogel **2** at 25°C: a) strain sweep at a frequency of 1 rad s^{-1}; b) time sweep at a strain of 0.1 % and frequency of 1 rad s^{-1}; c) frequency sweep at a strain of 0.1 %; d) temperature ramp at the heating rate of 1°C min^{-1}, strain of 0.1 % and frequency of 1 rad s^{-1}; time sweep at a strain of 0.1 % and frequency of 1 rad s^{-1}; f) viscosity as function of shear rate.

Time-dependent oscillation measurements can monitor the gelation process as hydrogel **2**, which forms gradually upon mixing of ligand **1** and Mg^{2+}. Time sweep shows the rapid growth of G' and G'' in the initial stage of gelation followed by a slower long term approach to final pseudo-equilibrium plateau (Figure 6b). At the end of the experimentation, the values of G' is about an order of magnitude higher than G''. Gel network formation obtained from time dependent oscillation is in correlation with the fluorescence studies, which show that maximum fluorescence intensity is reached at about 20 min.

Achievement of the aforementioned pseudo-equilibrium plateau allows for the implementation of a frequency sweep between 0.1 and 100 rad s^{-1} at the same temperature and within the LVR. This shows that $G' > G''$, confirming that the hydrogel **2** has predominantly an elastic character (Figure 6c). The elasticity of the gel is further evident from the fact that G' and G'' are minimally sensitive to Ω and the loss tangent (tan $\delta = G''/G'$) approaches a value of $\approx$0.1 in the tested frequency range. The double logarithmic plot of η^* (dynamic viscosity) versus ω (angular frequency) having gradient close to -1 [Note: $\eta^* = (G'^2 + G''^2)^{1/2}/\omega$], which is a characteristic of strong cohesive gel.[25]

The heating profile of hydrogel **2** during a controlled run at 1 °C min^{-1} from ambient temperature to 90 °C shows a sharp melting process between 70 and 75 °C indicative of "liquefaction" (Figure 6d). Subsequent cooling and isothermal run at 25 °C (Figure 6e) fail to recover the rigidity of the material prior to heating, with the viscous component being predominant. Though the gel is visually thermal reversible as mentioned before, the recovered gel is actually phase separated from the solvent. Hence, this implies that the morphology of hydrogel **2** is not entirely recoverable.

Besides the thermal effect, the response of hydrogel **2** to high shear fields will also determine its performance in potential applications. Increasing the rate of unidirectional shear from 0.01–1000 s^{-1} results in a reduction in the values of steady shear viscosity (shear thinning effect in Figure 6f). These are not recoverable within the opposite ramp thus exhibiting thixotropic behaviour for the hydrogel **2**, with a hysteresis loop forming between the forward and reverse pathway.

To further identify the linear/non-linear mechanical properties of hydrogel **2** at measuring times longer than $\approx$60 s employed maximally in Figure 6c, creep testing in the form of retarded and relaxed deformation has been utilised. Figure 7a reproduces the retardation and relaxation curves following careful application and removal of constant stress (5.0 Pa) for 60 min, respectively. Hydrogel **2** shows an instantaneous elastic response, characterised by an initial creep compliance, followed by a time-dependent creep region the slope of which gives the reciprocal of zero shear viscosity. At the final stage of the retardation curve, generated strain is about 1 % with the material remaining in the vi-

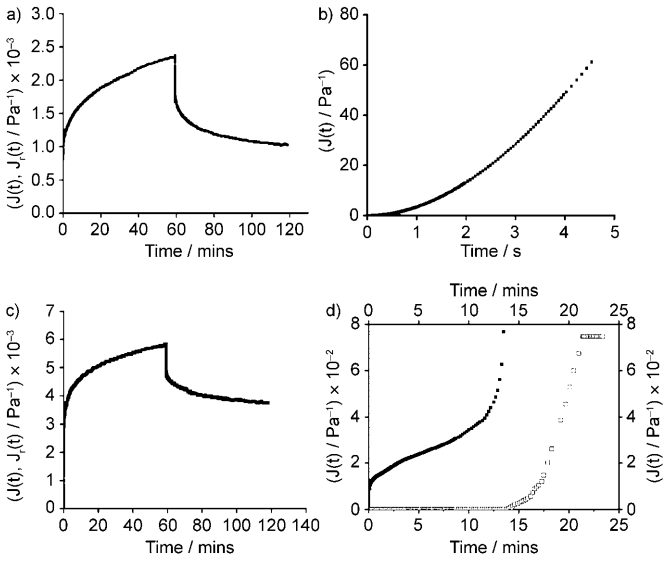

Figure 7. Creep retardation and recovery (relaxation) curves of hydrogel **2** at instantaneous stress of a) 5 Pa; b) 60 Pa; creep measurements of Zn^{2+} hydrogel c) 1 Pa; d) 1.5 Pa in which (■, primary axis) was a close-up of the complete curves (□, secondary axis).

cinity of LVR. Sudden removal of applied stress allows a reverse deformation that recovers 56% of the initial shape at the end of the relaxation curve. Higher application of stress (60 Pa) on the morphology of hydrogel **2** results in high levels of deformation (Figure 7b) and, consequently, the material is unable to recover its structure upon the subsequent relaxation experiment.

To compare the transient mechanical behaviour of hydrogel **2** with the closely related Zn^{2+} coordination polymeric gel,[12] creep retardation and relaxation measurements were also performed on the Zn^{2+} gel (Figure 7c,d). The retardation and relaxation curves following careful application and removal of constant stress (1.0 Pa) for 60 min, respectively is shown in Figure 7c. At the final stage of the retardation curve, angular displacement does not exceed 0.6% hence the material remains within LVR. Sudden removal of the constant stress allows a reverse deformation that recovers 35% of the initial material shape at the end of the relaxation curve. The effect of higher application of stress (1.5 Pa) on the integrity of Zn^{2+} gel is depicted in Figure 7d. Instantaneous deformation is followed by a diminishing rate of deformation change leading to a non-linear regime that reflects a catastrophic rearrangement of cross-links of the network. As a result there is infinitesimal recovery from the high ultimate extent of deformation during the subsequent relaxation experiment.

To quantify the long-time rearrangements in the matrix of Zn^{2+} hydrogel, the continuous pattern of flow that emerges following application of the instantaneous stress has been described by a discrete retardation spectrum. To facilitate comparisons between the two discrete applications of stress, a discrete exponential model of the experimental compliance, *J(t)*, was considered to be adequate.[26] Modelling provides the instantaneous compliance, J_o, the retarded compliance, J_1, the steady-state compliance, J_e, the retardation time of the Kelvin component, λ, and the steady shear viscosity. In brief, parameterization of the retardation data yields higher estimates of J_e (from 0.005–0.015 Pa^{-1}) with increasing values of applied stress (from 1.0–1.5 Pa). The transition from the small to large-deformation regime is also seen in the values of zero shear viscosity, which vary from ≈54–0.6 kPa s with increasing applications of stress. Finally, the irreversible rearrangement of cross-links is reflected in the λ values of the Kelvin component (spring and dashpot elements joined in series), which decrease from 3.4–0.4 s with increasing disintegration of the material.

Based on current mechanical evidence and results reported earlier in the literature,[12] it is evident that the three dimensional structure of hydrogel **2** is more cohesive than the Zn^{2+} gel. Thus, it is noticeable *that the G′* values of hydrogel **2** are about an order of magnitude higher than those of the Zn^{2+} gel. In addition, the melting temperature of hydrogel **2** is higher than for the Zn^{2+} gel (about 60 °C) arguing for a more thermally resistant network. As indicated by creep retardation testing, the Mg^{2+} gel sustained a high application of experimental stress and managed considerable levels of recovery. Applied stress as low as 1.5 Pa is capable of fracturing the Zn^{2+} hydrogel, whereas 40 times higher loads of stress are required for such catastrophic effect on the Mg^{2+} gel.

Comprehensive mechanical studies discussed here have exemplified the viscoelasticity of hydrogel **2**. The weak gel properties are resulted from the entanglement of coordination polymer and held together firmly by hydrogen-bonding interactions. Owing to the thixotropic behaviour, small deformation such as dynamic oscillation and steady shear allows recovery of hydrogel network by self assembly. Transient creep measurements further demonstrate the high recovery of the hydrogel **2**. This characteristic may enable the hydrogel in practical use.

Conclusion

We have demonstrated the hydrogelation properties of Mg^{2+} coordination polymer of muala anion. The gelation could be rationalised by the 1D coordination polymeric aggregate upon complexation of Mg^{2+}. This would facilitate the formation of fibrous nanostructures, which further self-assembles into a 3D-network structure through noncovalent interactions to entrap the water. The photophysical studies have shown that the hydrogel exhibits a typical π–π* transition and gives rise to high fluorescence behaviour. Upon the formation of the coordination polymeric gel, the complex shows a pronounced fluorescence enhancement with a longer lifetime, as compared to the ligand. A complementary armoury of dynamic oscillation, steady shear and transient experiments indicate the formation of a relatively strong and thermally resistant gel network, as compared to the corresponding Zn^{2+} hydrogel. The feasibility of Mg^{2+} hydrogel

as a free-standing fibre may find applications in flexible display devices. The strong blue emission of the hydrogel may be suitable for application in optoelectronic devices. The synthesised complexes and hydrogels may be biocompatible, as they are composed of Mg^{+} ions and an amino acid derivative, which makes them appropriate materials for biomedical applications.

Experimental Section

All starting materials were obtained commercially and used as received. The elemental analyses were performed in the microanalytical laboratory, Department of Chemistry, National University of Singapore. ^{1}H NMR spectra were recorded by using a Bruker ACF 300 spectrometer operating in the quadrature mode at 300 MHz. The infrared spectra (KBr pellet) were recorded by using an FTS165 Bio-Rad FTIR spectrophotometer in the range of $\tilde{\nu}=4000$–$400\,cm^{-1}$. ESI mass spectra were recorded by using a Finnigan MAT LCQ mass spectrometer by using the syringe pump method. Solvent present in the compounds was determined by using an SDT 2960 TGA thermal analyzer with a heating rate of 5°C min^{-1} from room temperature to 600°C. The UV/vis absorption spectra were obtained by using a Shimadzu UV2501-PC equipped with a temperature circulator. The gel samples were sandwiched between quartz plates. The fluorescence spectra were obtained from Perkin–Elmer LS 55 luminescence spectrometer equipped with a temperature circulator. Fluorescence lifetimes were measured by using time-correlated single-photon counting technique. The frequency-doubled output of a mode-locked Ti:-Sapphire laser (Tsunami, Spectra-Physics) was used for excitation of the sample at $\lambda=400$ nm. In fluorescence lifetime measurements, the fluorescence signal was collected by an optical fibre, which is directed to an avalanche photodiode (APD). The signals were processed by a PicoHarp 300 module (PicoQuant). The decay time profile was monitored at a wavelength of $\lambda=450$ nm. The system gives a temporal resolution of $\approx$100 ps.

Ligand H_2muala, **1** was synthesised according to the literature method.[27]

Synthesis of hydrogel [Mg(muala)(H_2O)$_2$]·*n*H_2O (2): To H_2muala (54.5 mg, 0.2 mmol) in LiOH (10 mg, 0.4 mmol) in water (2 mL), Mg(CH_3COO)$_2$·4H_2O (42.8 mg, 0.2 mmol) in water (2 mL) was added. The hydrogel is formed $\approx$20 min upon standing in ambient temperature. The solid powder of **2** can be obtained by slow evaporation methanolic solution. Mg(muala)(H_2O)(CH_3OH)$_{0.5}$ Yield: 25 mg, (40%). ^{1}H NMR (D_2O, 300 MHz): $\delta=7.47$ (d, 1H, Ar), 6.64 (d, 1H, Ar), 5.87 (s, 1H, Ar), 4.17 (d, 2H, -CH_2NH), 3.52 (q, 1H, -NHCH_2), 2.32 (s, 3H, -ArCH_3), 1.51 ppm (d, 3H, -CH_3); IR (KBr): $\tilde{\nu}=3430$ (OH), 3148 (NH), 1686 (COO^-), 1583 (COO^-) and 1392 cm^{-1} (CO); IR for freeze dried sample (KBr): $\tilde{\nu}=3415$ (OH), 1697 (COO^-), 1584 (COO^-) and 1396 cm^{-1} (CO); ESI-MS: 358.2 [Mg(muala)(H_2O)$_3$+H]$^+$; weight loss as per TGA: 9.7% (calculated for H_2O and CH_3OH: 10.2%); elemental analysis calcd (%) for $MgC_{14.5}H_{17}NO_{5.5}$: C 52.21, H 5.14, N 4.20; found: C 52.21, H 5.50, N 4.08.

Electron micrographs: Scanning electron microscopy (SEM) images were taken by using a Jeol JSM-6700F field emission scanning electron microscope operated at 5 kV and 10 μA. High resolution transmission electron microscopy (TEM) images and electronic diffraction patterns were obtained by using a JEOL JSM-3010 instrument.

Rheological measurements: These were carried out on freshly prepared gels using a controlled stress rheometer (AR-1000N, TA Instruments Ltd., New Castle, DE, USA). Parallel plate geometry of 40 mm diameter and 1.5 mm gap was employed throughout. Following loading, the exposed edges of samples were covered with a silicone fluid from BDH (100 cs) to prevent water loss. Dynamic oscillatory work kept a frequency of 1 rad s^{-1}. The following tests were performed: increasing amplitude of oscillation up to 200% apparent strain on shear, time and frequency sweeps at 25°C (60 min and from 0.1–100 rad s^{-1}, respectively), and a heating run to 90°C at a scan rate of 1°C min^{-1}. Unidirectional shear routines were performed at 25°C covering a shear-rate regime between 10^{-1} and 10^3 s^{-1}. Mechanical spectroscopy routines were completed with transient measurements. In doing so, the desired stress was applied instantaneously to the sample and the angular displacement was monitored for 60 min (retardation curve). After completion of the run, the imposed stress was withdrawn and the extent of structure recovery was recorded for another 60 min (relaxation curve). Dynamic and steady shear measurements were conducted in triplicate and creep (transient) measurements in duplicate.

Acknowledgement

We thank the Ministry of Education, Singapore for funding this project through NUS FRC Grant no. R-143-000-283-112. We are grateful to Prof. Vivian Wing-Wah Yam, University of Hong Kong for useful advice. We are thankful to Mr. Lakshminarayana Polavarapu and Dr. Xu Qing-Hua for helping fluorescence lifetime measurements.

[1] a) P. Terech, R. G. Weiss, *Chem. Rev.* **1997**, *97*, 3133–3160; b) R. G. Weiss, P. Terech, *Molecular Gels: Materials with Self-Assembled Fibrillar Networks*, Springer, Dordrecht, **2006**; c) M. George, R. G. Weiss, *Acc. Chem. Res.* **2006**, *39*, 489–497; d) L. A. Estroff, A. D. Hamilton, *Chem. Rev.* **2004**, *104*, 1201–1218; e) N. M. Sangeetha, U. Maitra, *Chem. Soc. Rev.* **2005**, *34*, 821–836; f) T. Ishi-i, S. Shinkai, *Top. Curr. Chem.* **2005**, *258*, 119–160; g) A. R. Hirst, D. K. Smith, *Chem. Eur. J.* **2005**, *11*, 5496–5508; h) D. K. Smith, *Adv. Mater.* **2006**, *18*, 2773–2778.

[2] a) G. Bühler, M. C. Feiters, R. J. M. Nolte, K. H. Dötz, *Angew. Chem.* **2003**, *115*, 2599–2602; *Angew. Chem. Int. Ed.* **2003**, *42*, 2494–2497; b) H.-J. Kim, J.-H. Lee, M. Lee, *Angew. Chem.* **2005**, *117*, 5960–5964; *Angew. Chem. Int. Ed.* **2005**, *44*, 5810–5814; c) F. Fages, *Angew. Chem.* **2006**, *118*, 1710–1712; *Angew. Chem. Int. Ed.* **2006**, *45*, 1680–1682, and ref. therein; d) B. S. Luisi, K. D. Rowland, B. Moulton, *Chem. Commun.* **2007**, 2802–2804; e) J. K.-H. Hui, Z. Yu, M. J. MacLachlan, *Angew. Chem.* **2007**, *119*, 8126–8129; *Angew. Chem. Int. Ed.* **2007**, *46*, 7980–7983.

[3] a) B. Xing, M.-F. Choi, B. Xu, *Chem. Eur. J.* **2002**, *8*, 5028–5032; b) T. Tu, W. Assenmacher, H. Peterlik, R. Weisbarth, M. Nieger, K. H. Dötz, *Angew. Chem.* **2007**, *119*, 6486–6490; *Angew. Chem. Int. Ed.* **2007**, *46*, 6368–6371.

[4] a) S. i. Kawano, N. Fujita, S. Shinkai, *J. Am. Chem. Soc.* **2004**, *126*, 8592–8593; b) J. Liu, P. He, J. Yan, X. Fang, J. Peng, K. Liu, Y. Fang, *Adv. Mater.* **2008**, *20,* 2508–2511.

[5] K. Kuroiwa, T. Shibata, A. Takada, N. Nemoto, N. Kimizuka, *J. Am. Chem. Soc.* **2004**, *126*, 2016–2021.

[6] S. Ray, A. K. Das, A. Banerjee, *Chem. Mater.* **2007**, *19*, 1633–1639.

[7] a) M. Shirakawa, N. Fujita, T. Tani, K. Kaneko, S. Shinkai, *Chem. Commun.* **2005**, 4149–4151; b) M. Shirakawa, N. Fujita, T. Tani, K. Kaneko, M. Ojima, A. Fujii, M. Ozaki, S. Shinkai, *Chem. Eur. J.* **2007**, *13*, 4155–4162.

[8] A. Kishimura, T. Yamashita, T. Aida, *J. Am. Chem. Soc.* **2005**, *127*, 179–183.

[9] a) J. B. Beck, S. J. Rowan, *J. Am. Chem. Soc.* **2003**, *125*, 13922–13923; b) Y. Zhao, J. B. Beck, S. J. Rowan, A. M. Jamieson, *Macromolecules* **2004**, *37*, 3529–3531; c) Weng, J. B. Beck, A. M. Jamieson, S. J. Rowan, *J. Am. Chem. Soc.* **2006**, *128*, 11663–11672; d) Weng, A. M. Jamieson, S. J. Rowan, *Tetrahedron* **2007**, *63*, 7419–7431.

[10] a) F. Camerel, R. Ziessel, B. Donnio, C. Bourgogne, D. Guillon, M. Schmutz, C. Iacovita, J.-P. Bucher, *Angew. Chem.* **2007**, *119*, 2713–2716; *Angew. Chem. Int. Ed.* **2007**, *46*, 2659–2662; b) A. Y.-Y. Tam, K. M.-C. Wong, G. Wang, V. W.-W. Yam, *Chem. Commun.* **2007**, 2028–2030.

[11] T. Cardolaccia, Y. Li, K. S. Schanze, *J. Am. Chem. Soc.* **2008**, *130*, 2535–2545.

[12] W. L. Leong, A. Y.-Y. Tam, S. K. Batabyal, L. W. Koh, S. Kasapis, V. W.-W. Yam, J. J. Vittal, *Chem. Commun.* **2008**, 3628–3630.

[13] J.-S. Wu, W.-M. Liu, X.-Q. Zhuang, F. Wang, P.-F. Wang, S.-L. Tao, X.-H. Zhang, S.-K. Wu, S.-T. Lee, *Org. Lett.* **2007**, *9*, 33–36.

[14] a) D. H. Wilkins, *Talanta* **1960**, *4*, 182–184; b) G. M. Huitnik, H. Diehl, *Talanta* **1974**, *21*, 1193–1202.

[15] a) L.-J. Dai, G. Ritchie, D. Kerstan, H. S. Kang, D. E. C. Cole, G. A. Quamme, *Physiol. Rev.* **2001**, *81*, 51–84; b) H. C. Politi, R. R. Preston, *Neuroreport* **2003**, *14*, 659–668; c) F. I. Wolf, A. Torsello, A. Fasanella, A. Cittadini, *Mol. Aspects Med.* **2003**, *24*, 11–26; d) F. I. Wolf, *Sci. STKE* **2004**, *233*, 23; e) H. Rubin, *BioEssays* **2005**, *27*, 311–320.

[16] a) M. Suzuki, M. Yumoto, M. Kimura, H. Shirai, K. Hanabusa, *Chem. Eur. J.* **2003**, *9*, 348–354; b) Y. Zhang, H. Gu, Z. Yang, B. Xu, *J. Am. Chem. Soc.* **2003**, *125*, 13680–13681; c) Z. Yang, G. Liang, B. Xu, *Chem. Commun.* **2006**, 738–740; d) I. A. Coates, A. R. Hirst, D. K. Smith, *J. Org. Chem.* **2007**, *72*, 3937–3940; e) M. Suzuki, M. Yumoto, H. Shirai, K. Hanabusa, *Chem. Eur. J.* **2008**, *14*, 2133–2144; f) Z. Yang, B. Xu, *Chem. Commun.* **2004**, 2424–2425; g) K. J. C. van Bommel, C. v. d. Pol, I. Muizebelt, A. Friggeri, A. Heeres, A. Meetsma, B. L. Feringa, J. v. Esch, *Angew. Chem.* **2004**, *116*, 1695–1699; *Angew. Chem. Int. Ed.* **2004**, *43*, 1663–1667; h) A. R. Hirst, D. K. Smith, M. C. Feiters, H. P. M. Geurts, *Chem. Eur. J.* **2004**, *10*, 5901–5910; i) G. Pitarresi, P. Pierro, F. S. Palumbo, G. Tripodo, G. Giammona, *Biomacromolecules* **2006**, *7*, 1302–1310; j) D. Das, A. Dasgupta, S. Roy, R. N. Mitra, S. Debnath, P. K. Das, *Chem. Eur. J.* **2006**, *12*, 5068–5074; k) Q. Wang, Z. Yang, X. Zhang, X. Xiao, C. K. Chang, B. Xu, *Angew. Chem.* **2007**, *119*, 4363–4367; *Angew. Chem. Int. Ed.* **2007**, *46*, 4285–4289; l) A. Shome, S. Debnath, P. K. Das, *Langmuir* **2008**, *24*, 4280–4288.

[17] a) S. V. Vinogradov, T. K. Bronich, A. V. Kabanov, *Adv. Drug Delivery Rev.* **2002**, *54*, 135–147; b) J. C. Tiller, *Angew. Chem.* **2003**, *115*, 3180–3183; *Angew. Chem. Int. Ed.* **2003**, *42*, 3072–3075; c) A. Friggeri, B. L. Feringab, J. v. Esch, *J. Controlled Release* **2004**, *97*, 241–248; d) S. R. V. Tomme, G. Storm, W. E. Hennink, *Int. J. Pharm.* **2008**, *355*, 1–18.

[18] a) K. Y. Lee, D. J. Mooney, *Chem. Rev.* **2001**, *101*, 1869–1880; b) E. Eisenbarth, *Sci. Isr.–Technol. Advantages Advanced Engineering Materials* **2007**, *9*, 1051–1060; c) M. R. Hynd, J. N. Turner, W. Shain, *J. Biosci. Polymer Edn.* **2007**, *18*, 1223–1244.

[19] a) Y. Zhang, Z. Yang, F. Yuan, H. W. Gu, P. Gao, B. Xu, *J. Am. Chem. Soc.* **2004**, *126*, 15028–15029; b) L. Applegarth, N. Clark, A. C. Richardson, A. D. M. Parker, I. Radosavljevic-Evans, A. E. Goeta, J. A. K. Howard, J. W. Steed, *Chem. Commun.* **2005**, 5423–5425; c) N. Shi, H. Dong, G. Yin, Z. Xu, S. Li, *Adv. Funct. Mater.* **2007**, *17*, 1837–1843.

[20] a) G. B. Deacon, R. J. Philips, *Coord. Chem. Rev.* **1980**, *33*, 227–250; b) K. Nakamoto, *Infrared and Raman Spectra of Inorganic and Coordination Compounds*, Wiley, New York, **1986**, pp.191.

[21] a) K. H Drexhage in *Dye Lasers, Vol 1* (Ed: F. P. Schafer), Springer-Verlag, New York, **1990**, pp.155–200; b) R. D. H. Murray, J. Mendez, S. A. Brown, *The Natural Coumarins: Occurrence, Chemistry and Biochemistry*, Wiley, Chichester, **1982**.

[22] a) S. Y. Ryu, S. Kim, J. Seo, Y.-W. Kim, O.-H. Kwon, D.-J. Jang, S. Y. Park, *Chem. Commun.* **2004**, 70–71; b) F. Camerel, L. Bonardi, M. Schmutz, R. Ziessel, *J. Am. Chem. Soc.* **2006**, *128*, 4548–4549; c) P. Xue, R. Lu, G. Chen, Y. Zhang, H. Nomoto, M. Takafuji, H. Ihara, *Chem. Eur. J.* **2007**, *13*, 8231–8239.

[23] a) C. Bao, R. Lu, M. Jin, P. Xue, C. Tan, G. Liu, Y. Zhao, *Org. Biomol. Chem.* **2005**, *3*, 2508–2512; b) S. Manna, A. Saha, A. K. Nandi, *Chem. Commun.* **2006**, 4285–4287.

[24] S. Li, L. He, F. Xiong, Y. Li, G. Yang, *J. Phys. Chem. B*, **2004**, *108*, 10887–10892.

[25] S. Kasapis, I. M. Al-Marhoobi, M. Deszczynski, J. R. Mitchell, R. Abeysekera, *Biomacromolecules*, **2003**, *4*, 1142–1149.

[26] V. Kontogiorgos, H. D. Goff, S. Kasapis, *Biomacromolecules*, **2007**, *8*, 1293–1299.

[27] R. H. Mehta, *J. Indian Chem. Soc.* **1983**, *60*, 201.

Received: June 10, 2008
Published online: September 12, 2008

